A Comparative NMR Study on the Reactions of Hf(IV) Organometallic Complexes with Al/Zn Alkyls

Luca Rocchigiani,[*,†,‡,‖] *Vincenzo Busico,*[§,‡] *Antonello Pastore,*[§,‡] *and Alceo Macchioni*[†,‡]

[†]Dipartimento di Chimica, Biologia e Biotecnologie and CIRCC, Università degli studi di Perugia, Via Elce di sotto, 8, I-06123 Perugia, Italy. [§]Dipartimento di Scienze Chimiche, Università di Napoli Federico II, Via Cintia, I-80126 Napoli, Italy. [‡]Dutch Polymer Institute (DPI) PO box 902, 5600 AX Eindhoven, The Netherlands. [‖]Current address: School of Chemistry, University of East Anglia, Norwich NR4 7TJ, UK.

email: L.Rocchigiani@uea.ac.uk

ABSTRACT

NMR spectroscopy has been exploited to investigate the reactions of Hf(IV) organometallic complexes with trialkylaluminium and dialkylzinc, with the aim of obtaining insights into the elementary steps of coordinative chain transfer polymerization (CCTP). Bis-cyclopentadienyl hafnium dimethyl (Cp$_2$HfMe$_2$, **1Me$_2$**) and [N-[2,6-Diisopropylphenyl]-α-[2-isopropylphenyl]-6-(1-naphthalenyl)-2-pyridinemethanaminato]hafnium dimethyl (**2Me$_2$**) complexes have been chosen as case studies for understanding the differences between poorly performing and highly active CCTP catalysts, in an attempt to assess the effect of the ancillary ligand on the transalkylation rate. **2Me$_2$** was found to react much faster with both AlEt$_3$ and ZnEt$_2$ than **1Me$_2$**, mainly due to a remarkably lower activation enthalpy. In addition, while the ethylation rate was found to depend on the nature of the alkylating agent for **1Me$_2$**, it does not for **2Me$_2$**. This difference in reactivity was observed also in the case of the ion pairs obtained by reacting **1Me$_2$** and **2Me$_2$** with [CPh$_3$][B(C$_6$F$_5$)$_4$]. For the latter species, NMR indicated that two main deactivation pathways, namely anion decomposition and σ-bond methatesis of Hf-alkyl groups, occur.

Introduction

Chain transfer reactions between transition organometallic complexes and main element alkyls play a crucial role in homogeneous olefin polymerization catalysis.[1] Polymeryl-group migration from active sites to co-catalysts, most frequently aluminium alkyls or methylaluminoxane (MAO),[2,3] is indeed a suitable chain termination process that can be exploited in tuning molecular weight and end-group structures of resulting polyolefins.[4] This is particularly true in the case of living polymerization,[5] since chain transfer increases the number of chains produced by each catalytic site and decreases the polydispersity.[6] This concept is key in coordinative chain transfer polymerization (CCTP, Scheme

1

1),[7] a reaction protocol based on the addition of chain transfer agents, such as AlR$_3$, ZnR$_2$ or MgR$_2$, to the catalytic pool, aimed at stimulating fast and reversible alkyl exchange between active transition metal and main element. As a matter of fact, when CCTP conditions are attained, chain transfer occurs faster than monomer insertion ($k_{CT} \gg k_P$, Scheme 1) resulting in polymers with extremely narrow molecular weight distributions.[8]

From the mechanistic point of view, the key step of CCTP relies on the formation of binuclear adducts in which polymeryl groups act as bridges between transition metal and main metal centers (Scheme 1).[7] Despite rather intensive research in this area, little is known about adducts between active catalysts for CCTP and main metal alkyls, mainly due to their dynamic nature and low stability in solution. In a few cases, well defined $L_nM(\mu\text{-}R)_nER_m$ (M=transition metal, E=main metal) heterobimetallic adducts have been characterized, including group IV metallocenes,[9] rare earth-metal[10] or bis-iminopyridyl V,[11] Fe[12] and Co[13] complexes, but only when E=Al. Recently, we have shown that cationic pyridylamido Hf complexes,[14] which are remarkably active catalysts for CCTP,[8,15] react with zinc and aluminium alkyls to give heterobimetallic adducts. In the latter ones, the cyclometalated naphthyl group acts as a bridge between hafnium and main metal atoms, closely resembling the proposed intermediate for CCTP.[16] The investigation of degenerative alkyl transfer kinetics revealed that Hf/Zn methyl exchange was faster than Hf/Al one, suggesting that the nature of metal alkyl is key in tuning the fluxionality of such adducts.
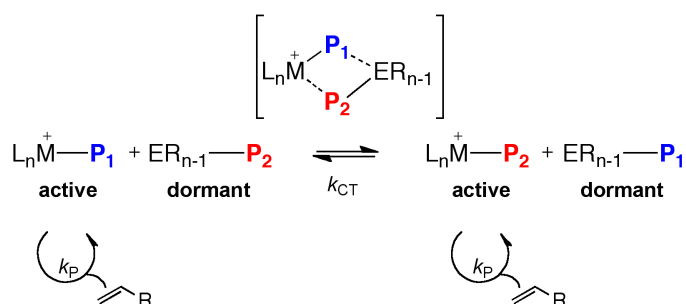
Scheme 1. Mechanism of coordinative chain transfer polymerization (M= transition metal, E=main element).

Nuclear Magnetic Spectroscopy has proven to be a suitable technique for mechanistic investigations of homogeneous olefin polymerization[17] and, in the present study, we exploited NMR for studying the reactivity of biscyclopentadienyl- and (pyridylamido)hafnium complexes with ZnR$_2$ and AlR$_3$ (R=Me or Et). The main purpose of this work is to compare the behavior of the simplest hafnocene Cp$_2$HfMe$_2$ (**1Me$_2$,** Scheme 2), which is not a suitable catalyst for chain transfer polymerization, with that of the highly optimized pyridylamido complex (**2Me$_2$**, Scheme 2) that is one of the most effective group IV catalysts in CCTP. First, we investigated the reactivity of mixtures containing ZnEt$_2$ and AlEt$_3$. Secondly, a kinetic study of their reactions with hafnium dimethyl species was car-

ried out for evaluating the effect of the ancillary ligand on the activation parameters. Then, the reactivity of Zn– and Al–alkyls with cationic metallocenium species was explored and compared to that of the previously reported pyridylamido cationic complexes. Finally, the thermal decomposition of pyridylamido-Zn/Al heterobimetallic adducts was studied for understanding the role of chain transfer agent in deactivating the catalytic system.
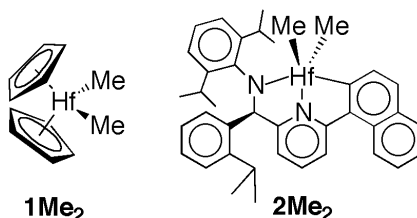

Scheme 2. Hafnium complexes considered in this study.

Results and discussion

1. AlEt$_3$/ZnEt$_2$ mixtures

^{1}H and ^{13}C NMR spectra of a 1:1 AlEt$_3$/ZnEt$_2$ mixture in toluene-d_8 showed the presence of only one set of signals at room temperature, having chemical shift values equal to the average of those of pure components. This indicates that a fast ethyl exchange process between aluminum and zinc atoms does occur, as already reported for AlMe$_3$/ZnMe$_2$ mixtures.[18] Nevertheless, at low temperature the process became slow with respect to the NMR timescale and three different sets of signals separated below 200 K (Figure 1a); they were assigned to *a)* the ethyl group bound to the Zn atom [δ_H(CH$_2$)=0.09 ppm], *b)* the terminal [δ_H(CH$_2$)=0.16 ppm and *c)* the bridging [δ_H(CH$_2$)=0.67 ppm] ethyl groups of the AlEt$_3$ dimer.[19] The simulation of the VT NMR spectra was hampered by the presence of many signals with different populations and only approximate rate constant values for alkyl exchange were derived in this specific case. For example, coalescence between unbridging methylene signals of AlEt$_3$ and ZnEt$_2$ was detected at 210 K and an approximate rate constant of 70 s^{-1} was calculated ($\Delta G^{\neq}$=10.3 kcal/mol).[20]
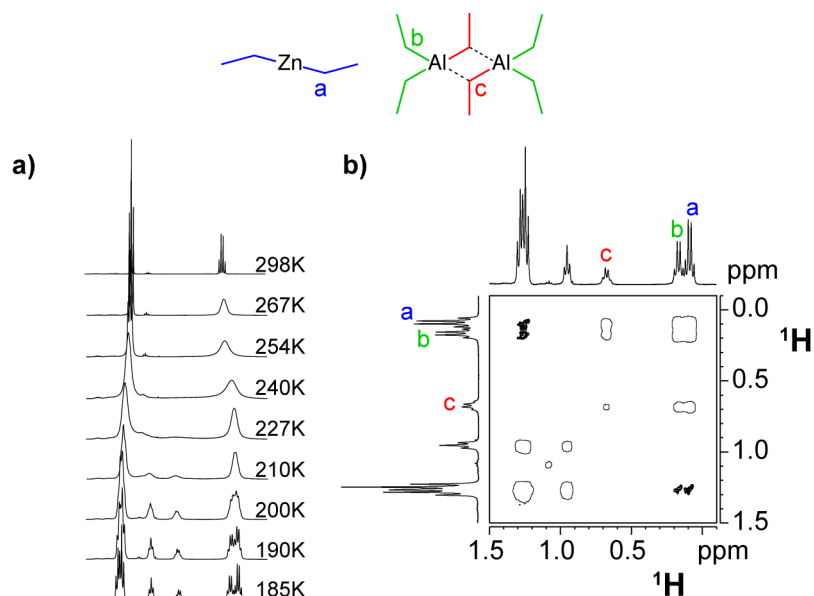
Figure 1. a) VT ^{1}H NMR spectra of a 1:1 mixture of AlEt$_3$ and ZnEt$_2$ in toluene-d_8; b) ^{1}H NOESY NMR spectrum recorded at 185 K.

At 185 K, the ^{1}H NOESY NMR spectrum of the mixture (Figure 1b) showed the presence of intense exchange cross peaks, revealing that the alkyl exchange occurs also at rather low temperatures. Interestingly, the bridging ethyl groups of AlEt$_3$ dimer were in exchange with both terminal and Zn-ethyl groups, likely owing to the dissociation/recombination process of the Al dimer.[18a,19] Additionally, the uniform signal broadening with temperature observed in VT ^{1}H NMR spectra suggested the presence of a unique kinetic constant for all the exchanges. This could be explained assuming the dissociation of the AlEt$_3$ dimer as rate determining step, as already suggested for the AlR$_3$/GaR$_3$ exchange.[18a]

2. 1Me$_2$/ER$_n$ mixtures

The reaction of **1Me$_2$** with an excess of ZnEt$_2$ or AlEt$_3$ in benzene-d_6 led to the formation of Cp$_2$HfMeEt (**1MeEt**) and Cp$_2$HfEt$_2$ (**1Et$_2$**, Scheme 3), as indicated by the appearance of two overlapped signals at δ_H=1.45 ppm ($^3J_{HH}$=7.8 Hz, $^1J_{C,H}$=124.6 Hz) in the ^{1}H NMR spectrum. They were assigned to the CH$_3$ groups of the Hf-ethyl moieties, in agreement with previous observations.[21]
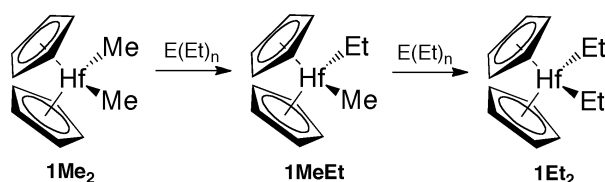
Scheme 3. Ethyl transfer from E(Et)$_n$ to **1Me$_2$**.

In contrast with zirconocenes,[21] ethyl transfer reactions occur slowly at room temperature. For instance, 80% conversion of **1Me$_2$** into **1MeEt** and **1Et$_2$** was obtained after 17 hours in the presence of 30 equivalents of ZnEt$_2$ at room temperature. **1Me$_2$** was instead consumed in approximately 85 minutes when 2 equivalents of AlEt$_3$ were used (Figure 2). Ethylated hafnocenes showed to be remarkably stable in solution up to 350 K, even if traces of ethane (δ_H=0.80 ppm) were detected during the reactions, in particular at temperatures above 320 K.
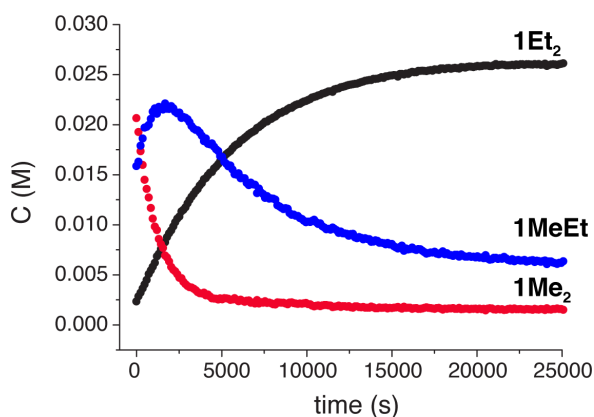
Figure 2. Concentration *versus* time plot obtained for the reaction of **1Me$_2$** with 2 equivalents of AlEt$_3$ in toluene-d_8 at 298 K.

Kinetic profiles of methyl-to-ethyl transalkylation at variable temperature were obtained by following the evolution of the ^{1}H NMR spectra with time, as depicted in Figure 2. By a qualitative analysis, it is possible to note that the first ethylation is markedly faster than the second one and the concentration of **1MeEt** shows a maximum that is dependent on both temperature and Hf/ER$_n$ ratio. These observations are consistent with a consecutive reaction pathway, in which **1Et$_2$** is formed only from **1MeEt** and not owing to a double ethylation of **1Me$_2$**.

Table 1 collects kinetic constants obtained for first (k_1) and second (k_2) alkylation of **1Me$_2$** with ZnEt$_2$ and AlEt$_3$ at different reaction temperatures (Experimental Section for details). The results show that the first alkyl exchange reaction is 2-4 times faster than the second, independent of the alkylating agent. On the other hand, the main group metal plays a crucial role since reactions with AlEt$_3$ are notably faster than those with ZnEt$_2$. As an example, at 300K kinetic constants obtained in the case of aluminium are twenty times larger than those obtained with zinc.

Table 1. Second-order rate constants (M^{-1} s^{-1}) for first (k_1) and second (k_2) ethylation of **1Me$_2$** obtained at different temperatures (K) with different alkylating agents.

	ZnEt$_2$		AlEt$_3$	
T	k_1	k_2	k_1	k_2
267.5	-	-	$(6.6\pm0.2)\cdot10^{-5}$	$(2.7\pm0.2)\cdot10^{-5}$
273.8	-	-	$(1.5\pm0.3)\cdot10^{-4}$	$(4.9\pm0.8)\cdot10^{-5}$

287.3	-	-	$(4.9\pm0.6)\cdot10^{-4}$	$(1.8\pm0.1)\cdot10^{-4}$
300.1	$(7.5\pm0.6)\cdot10^{-5}$	$(3.1\pm0.3)\cdot10^{-5}$	$(1.6\pm0.2)\cdot10^{-3}$	$(5.5\pm1.8)\cdot10^{-4}$
320.6	$(4.1\pm0.6)\cdot10^{-4}$	$(1.0\pm0.2)\cdot10^{-4}$	-	-
342.4	$(2.4\pm0.4)\cdot10^{-3}$	$(5.2\pm0.9)\cdot10^{-4}$	-	-
349.5	$(4.1\pm0.7)\cdot10^{-3}$	$(8.5\pm1.3)\cdot10^{-4}$	-	-

The Eyring analysis of k_1 values (Figure 3) allowed the transalkylation activation parameters to be determined. In the case of $ZnEt_2$, the activation enthalpy is equal to 16.2 ± 0.3 kcal/mol and the activation entropy amounts to -22 ± 1 cal/mol·K while, for $AlEt_3$, a similar $\Delta S^{\neq}$ (-23 ± 2 cal/mol·K) and a lower $\Delta H^{\neq}$ (14.6 ± 0.5 kcal/mol) are obtained.
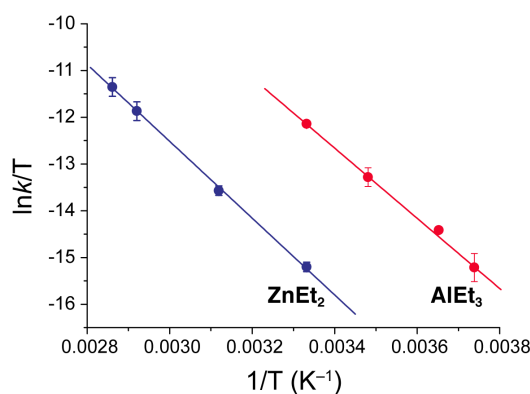
Figure 3. Eyring plots for the ethylation of **1Me$_2$** with $ZnEt_2$ and $AlEt_3$ in toluene-d_8.

In the case of Al-alkyls, the complication derived from the formation of Al_2R_6 dimers, which might affect the trans-alkylation kinetics, has to be taken into account. For this reason, reactions of **1Me$_2$** with variable amounts of $AlEt_3$ (1:1, 2:1 and 4:1 Al/Hf ratios) were performed. The kinetic model was modified slightly to take into account possible equilibrium effects ascribed to the lower concentration of $AlEt_3$. Interestingly, rate constant values at 298K are three times larger when hafnocene and aluminium alkyl are equimolar ($k_1=4.83\cdot10^{-3}$ M^{-1} s^{-1}) while decrease by increasing the concentration of $AlEt_3$ to reach a plateau at an Al/Hf ratio between 5 and 10 (Supporting Information).

It was also considered worthwhile to perform a reaction between **1Me$_2$** and a mixture of $ZnEt_2$/$AlEt_3$ in a 1:1:1 molar ratio, with the aim of exploring the role of the fast ethyl exchange between Zn and Al atoms in the alkylation of the transition metal complex. The quantification of the kinetic rate constants gave a k_1 value of $2.4\cdot10^{-3}$ M^{-1} s^{-1}, which is quite similar to the values obtained in the experiment with only $AlEt_3$ at lower Al/Hf ratios (Supporting Information).

The analysis of the results reveals that the ethylation of **1Me$_2$** by $ZnEt_2$ and $AlEt_3$ is a slow reaction with a rather high activation barrier ($\Delta G^{\neq}=22.7$ and 21.4 kcal/mol for $ZnEt_2$ and $AlEt_3$, respectively) that is composed by a large activation enthalpy (16.2 kcal/mol for $ZnEt_2$ and 14.6 kcal/mol for $AlEt_3$) and a negative activation entropy (-22 and -23 cal/mol·K for $ZnEt_2$ and $AlEt_3$, respectively).

The latter values fit nicely with previously reported data on degenerative methyl transfer between **1Me₂** and AlMe₃[22] and are consistent with an associative mechanism, in which the main element alkyl and metallocene form a heterobimetallic complex featuring one or more bridging alkyl groups. Since similar $\Delta S^{\neq}$ values were measured for ZnEt₂ and AlEt₃, it is reasonable to assume that the reaction pathway is the same for both. Moreover, the activation entropy value points out that the dissociation/recombination of AlEt₃ dimer is not rate determining. AlEt₃ dimerization has a modest detrimental effect, as deduced by the slightly higher reaction rates at lower Al/Hf ratios, likely due to a higher amount of Al₂Et₆ dimers that dissociate to monomeric AlEt₃, thus increasing the alkylation efficiency. Concerning the activation enthalpy, the lowest $\Delta H^{\neq}$ value observed for AlEt₃ ($\Delta\Delta H^{\neq}_{(Zn-Al)}=1.6$ kcal/mol) could be related to the higher tendency of the latter of forming dimers with metallocenes and stronger E–Me bonds.[23] The associative transition state should be, in effect, stabilized by Hf–(μ-Me)–ERₙ bridges, whose formation is preferred with Al-alkyls.

Finally, the results obtained on the ethylation of **1Me₂** with a 1:1 AlEt₃/ZnEt₂ mixture are coherent with the proposed mechanistic scenario. The observation of reaction rates similar to those measured with pure AlEt₃ confirms that *i)* the Al/Zn ethyl exchange is not rate determining and *ii)* there are no cooperative effects, so that the reaction rate is determined by the alkylation of the most efficient metal–alkyl.

3. 2Me₂/ERₙ mixtures

The reaction of **2Me₂** with 1 equivalent of ZnEt₂ in benzene-d_6 afforded a mixture of stable mono- and bis-ethylated complexes, as seen above for **1Me₂**. Four different Hf–ethyl groups were observed in the ¹H NMR spectrum, with methyl groups resonating at $\delta_H=1.75$, $\delta_H=1.72$, $\delta_H=1.53$ and $\delta_H=1.44$ ppm ($^3J_{HH}=8.0$ Hz). They were assigned to *i)* the two diastereotopic (*anti* and *syn* with respect to the 2-(Me₂CH)-C₆H₄ substituent) Hf–Et moieties of **2Et₂** and *ii)* the ethyl groups of the two equally populated diastereoisomeric **2MeEt** species (Scheme 4). When 1 equivalent of AlEt₃ was used, the same reactivity was observed. However, some resonances of reaction products appeared slightly broadened, likely due to dynamic processes. Contrary to what was observed with ZnEt₂, the reaction mixture was unstable at room temperature and slow decomposition of AlEt₃ to ethane occurred.
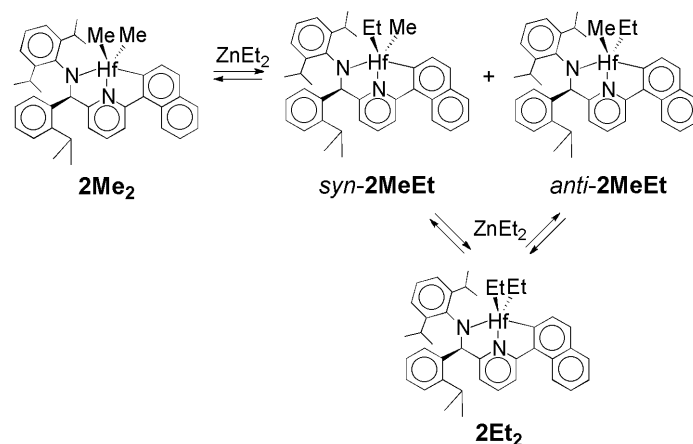
Scheme 4. Transalkylation reaction between **2Me₂** and ZnEt₂.
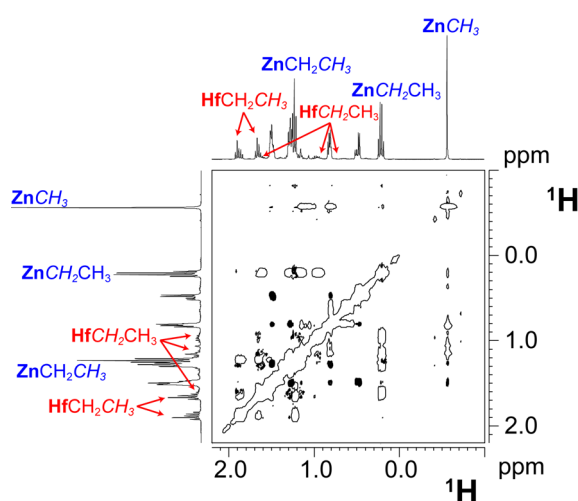
Figure 4. A section of the ^{1}H NOESY NMR spectrum of the mixture obtained after the reaction of **1Me₂** with ZnEt₂ (benzene-d_6, 297 K).

As far as the reaction rate was concerned, alkyl exchange was very fast with both ZnEt₂ and AlEt₃ and it was not possible to follow the ethyl transfer by ^{1}H NMR spectroscopy. Nevertheless, the phase sensitive ^{1}H NOESY NMR spectrum of the reaction mixture (Figure 4, ER$_n$=ZnEt₂) revealed the presence of exchange cross peaks between Zn/Al–alkyl and Hf–alkyl resonances, indicating that a fast and reversible transalkylation occurs at equilibrium. This prompted us to explore the reaction kinetics by means of variable temperature ^{1}H EXSY NMR,[24] with the aim of obtaining activation parameters to compare with those measured for the reactions of **1Me₂**.

The kinetic study was performed by using a 5-fold excess of ER$_n$, in order to promote the exclusive formation of **2Et₂** and simplify the NOE spectra (Supporting Information). No exchange between *anti* and *syn* ethyl groups of **2Et₂** was detected, indicating that the interconversion of the two alkyls on the metal center is very slow (or frozen), as also observed for **2Me₂**. Second order kinetic rate constants were determined from ^{1}H EXSY spectra taking into account the different populations of

the exchanging sites (Experimental Section). In the case of AlEt₃, the temperature window was limited by decomposition, which is faster than the measurement time above 300 K.

Table 2. Second order rate constants ($M^{-1}\,s^{-1}$) for the reversible transalkylation of *syn* (k_{syn}) and *anti* (k_{anti}) ethyl groups of **2Et₂** with ZnEt₂ (C_{Hf}=32.0 mM, Zn/Hf=6) and AlEt₃ (C_{Hf}= 34.0 mM, Al/Hf=5) at different temperatures (T, K).

T	ZnEt₂		AlEt₃	
	k_{syn}	k_{anti}	k_{syn}	k_{anti}
273.8	-	-	1.5±0.1	2.8±1.2
287.3	-	-	3.4±0.1	5.4±1.5
300.1	3.1±0.1	3.5±0.8	-	-
300.8	-	-	7.1±0.3	11.2±1.4
320.6	6.2±0.3	7.1±1.3	-	-
335.6	9.7±0.3	11.6±4.6	-	-
349.6	15.8±2.7	19.3±7.2	-	-

The results reported in Table 2 show that the rate constants of the reversible transalkylation of **2Et₂** are notably larger than those measured for irreversible hafnocene ethylations. For example, at 300 K the reversible ethyl exchange with ZnEt₂ is four orders of magnitude faster than the methyl to ethyl exchange of **1Me₂**. Moreover, transalkylation of the two ethyl groups in *syn* and *anti* positions occurs essentially with the same reaction rate, indicating that the process is not diastereoselective. The behavior of AlEt₃ and ZnEt₂ is not markedly different; for example, at 300 K rate constant values measured with AlEt₃ are only 2-3 times larger than those obtained with ZnEt₂.

The Eyring analysis of average transalkylation rate constants (Supporting Information) provided an activation enthalpy of 6.3±0.3 kcal/mol for ZnEt₂ and 8.1±0.3 kcal/mol for AlEt₃. For the activation entropy, values of –35±2 and –27±2 cal·mol/K were obtained for ZnEt₂ and AlEt₃, respectively.

The effect of AlEt₃ concentration was explored by performing ¹H EXSY NMR experiments at different concentrations of hafnium complex and AlEt₃ keeping their molar ratio constant, in order to induce the full conversion of **2Me₂** and **2MeEt** to **2Et₂**. The results showed that, for **2Et₂** at a concentration of 9.5 mM, average rate constants of reversible transalkylation were only 2 times larger than those measured at 34.0 mM (Figure 5). The Eyring analysis of such data allowed a $\Delta H^{\neq}$ of 7.5±0.3 kcal/mol and a $\Delta S^{\neq}$= –28±3 cal·mol/K to be derived (Supporting Information).

When **2Me₂** was mixed with 1 equivalent of AlEt₃ and 10 equivalents of ZnEt₂, the trend of rate constants was similar to that obtained for pure ZnEt₂ (Figure 5). For example, the average rate constant measured at 300 K is 4.2 $M^{-1}s^{-1}$, while that of pure ZnEt₂ is 3.3 $M^{-1}s^{-1}$ at the same temperature.
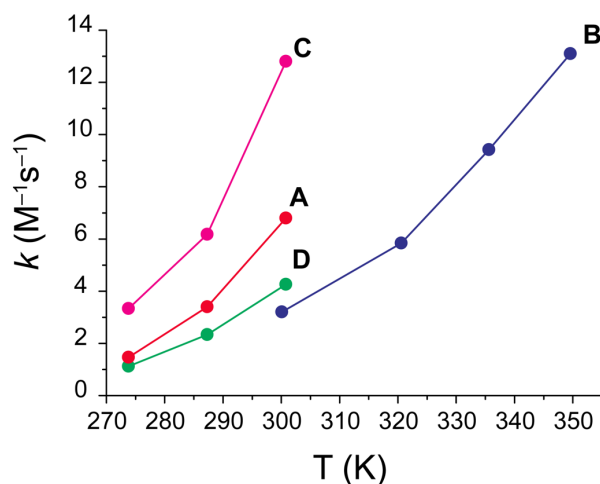
Figure 5. Second order rate constants (k, $M^{-1}s^{-1}$) for reversibile transalkylation of **2Et$_2$** with AlEt$_3$ (A: C_{Hf}=34.0 mM, Al/Hf=5; C: C_{Hf}=9.5 mM, Al/Hf=5), ZnEt$_2$ (B: C_{Hf}=34.0 mM, Zn/Hf=6) and their mixture (D: C_{Hf}=37.9, Zn/Al/Hf=10:1:1) in toluene-d_8.

To summarize, it was shown that **2Et$_2$** undergoes fast and reversible ethyl exchange with ER$_n$. Contrary to what observed for cationic species,[16] cyclometalated naphthyl group does not give ligand exchange with Al/Zn alkyls, suggesting that a coordinative vacancy is necessary to promote the breakage of the Hf–aryl bond. The free activation energy at 298K for reversible ethyl exchange is close to 16.0 kcal/mol for both the alkylating agents. The activation barrier is composed of a large and negative activation entropy (–27 and –35 cal·mol/K for AlEt$_3$ and ZnEt$_2$, respectively) and a modest activation enthalpy (8.1 and 6.3 kcal/mol for AlEt$_3$ and ZnEt$_2$, respectively). $\Delta S^{\neq}$ values suggest an associative mechanism in which the alkyl is exchanged through the formation of a heterobimetallic adduct at the transition state, as previously inferred above for **1Me$_2$**. Also in the present case, $\Delta S^{\neq}$ values measured for AlEt$_3$ and ZnEt$_2$ are not markedly different thus indicating that the dissociation/recombination process of AlEt$_3$ is not rate determining. Higher values of activation enthalpy were obtained for AlEt$_3$ ($\Delta\Delta H^{\neq}$=1.8 kcal/mol), in contrast to those observed with **1Me$_2$**. This could be due to the higher Lewis acidity of the Hf atom in the pyridylamido complex that prevents the dimerization with AlEt$_3$ through the establishment of bridging interactions. In such a mechanistic scenario, the more electron-rich ZnEt$_2$ could be favored in the interaction with the postmetallocene complex and undergo transalkylation with a lower activation enthalpy.

4. Metallocenium species/ER$_n$ mixtures

The reactivity of cationic hafnocenes with ER$_n$ was explored using both mononuclear [Cp$_2$HfMe][B(C$_6$F$_5$)$_4$] and binuclear [(Cp$_2$HfMe)$_2$(μ-Me)][B(C$_6$F$_5$)$_4$] [**1(μ-Me)1**] ion pairs, which can be straightforwardly obtained by reacting **1Me$_2$** with 1 or 0.5 equivalents of [CPh$_3$][B(C$_6$F$_5$)$_4$], respectively. The mononuclear ion pair quickly underwent –C$_6$F$_5$ transfer reactions, especially when Zn al-

kyls were used. Therefore, the attention was focused on **1(μ-Me)1** that, despite it is not likely relevant under polymerization conditions, allowed us to probe collateral reactions occurring at the metal center and tendency of ER_n to split hafnocenium dimers.

a) Reactions with AlMe₃. When a 10-fold excess of $AlMe_3$ was added to a solution of **1(μ-Me)1** in toluene-d_8, the ^{1}H NMR spectrum of the reaction mixture showed the immediate consumption of the starting hafnium complex and the concomitant formation of two new species in a 1:1 ratio that were assigned to **1Me₂** and $[Cp_2Hf(\mu\text{-Me})_2AlMe_2][B(C_6F_5)_4]$[9f] [**1(μ-Me)Al**]. The ^{1}H NOESY NMR spectrum of the reaction mixture (Figure 6a) revealed the presence of a selective pattern of chemical exchange involving: *i)* the cyclopentadienyl rings of both neutral and ionic metallocenes, *ii)* the methyl groups of **1Me₂** and the brigding ones of **1(μ-Me)Al**, *iii)* the terminal methyl moieties of **1(μ-Me)Al** and free $AlMe_3$. In line with previous observations,[25] no exchange was detected between terminal and bridging methyl groups of the bimetallic cation in the 298–338 K temperature range, thus indicating that the $AlMe_3$ dissociation/recombination in **1(μ-Me)Al** is very slow (or frozen). Further evidence of this was obtained from a ^{19}F,^{1}H HOESY NMR experiment, which showed the presence of dipolar contacts between the fluorine atoms of the borate anion and the methyl groups of **1Me₂** (Figure 6b) likely due to transferred Overhauser Effect.[26]
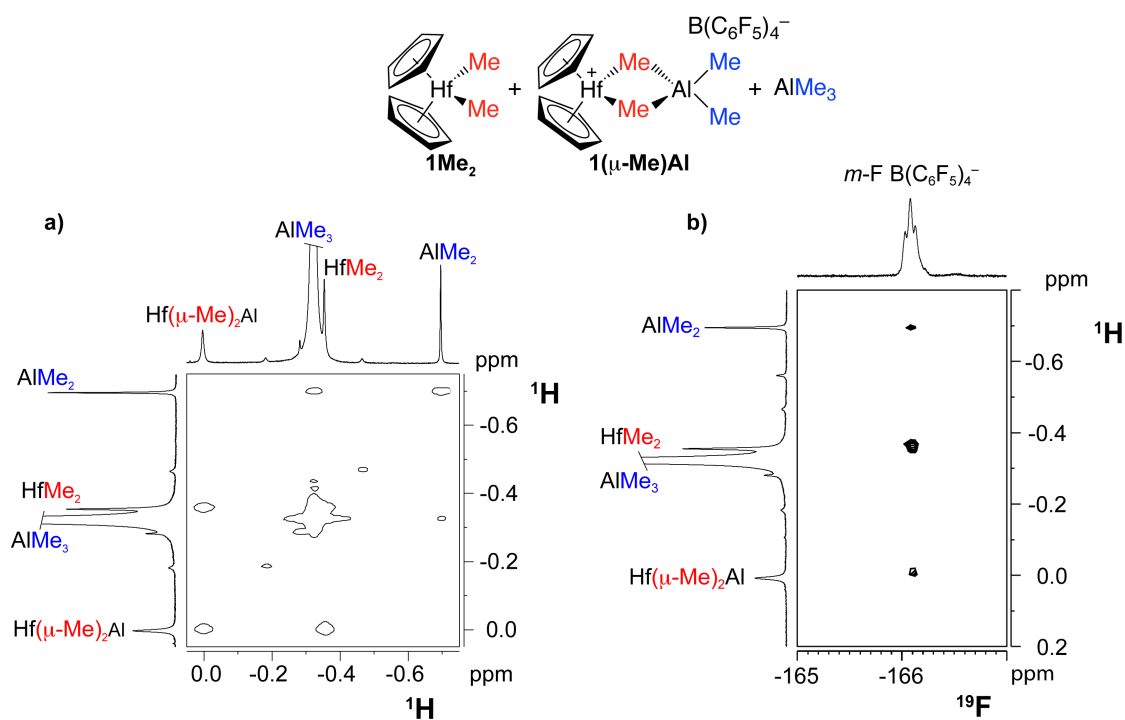
Figure 6. a) A section of the ^{1}H NOESY NMR spectrum of a toluene-d_8 solution containing **1Me₂**, **1(μ-Me)Al** and AlMe₃; b) a section of the ^{19}F,^{1}H NOESY NMR spectrum of the same mixture.

The timescale of fluxionality was suitable for VT ^{1}H EXSY NMR experiments and kinetic rate constants were determined by applying a two-site exchanging model.[24] The results are reported in

Table 3 and show that the exchange of hafnium methyl groups occurs roughly 20 times faster than those of aluminum along the explored temperature range. The Eyring analysis of the data afforded $\Delta H^{\neq}$ values of 13.7±1.0 and 14.1±1 kcal/mol for the Hf–Me and Al–Me exchanges, respectively, while $\Delta S^{\neq}$ values of –8±1 and –14.0±1 cal·mol/K were obtained.

Formally, the observed dynamic process suggests that $[AlMe_2][B(C_6F_5)_4]$ ion pairs[27,28] are exchanged between neutral and ionic metallocenes. The obtained activation entropy values indicate that the reaction occurs via associative interchange, likely through the attack of **1Me₂** at the Al atom of the bimetallic **1(μ-Me)Al** ion pair; the same conclusion applies to the exchange with $AlMe_3$, for which similar $\Delta H^{\neq}$ and $\Delta S^{\neq}$ were obtained. Activation enthalpy values are rather high for both processes and similar to those obtained in the case of the ethyl exchange on neutral hafnocenes, indicating that such processes are still difficult on cationic species, presumably due to the strong $AlMe_3$– hafnocene bridging interaction and the large Hf–Me bonding energy.

**Table 3.** Rate constants (M^{-1} s^{-1}) for **1Me₂**/**1(μ-Me)Al** (k_1) and **1(μ-Me)Al** /$AlMe_3$ (k_2) reversible exchanges as a function of temperature (T, K).

T	k_1	k_2
298	(8.1±0.8)	(0.2±0.1)
308	(20.0±2.0)	(0.8±0.2)
318	(42.6±0.2)	(1.3±0.1)
328	(74.2±0.4)	(2.6±0.1)
338	(152.0±3.0)	(4.9±0.1)

b) Reactions with ZnMe₂. Upon mixing a solution of **1(μ-Me)1** in toluene-d_8 with 5 equivalents of $ZnMe_2$, no sign of reaction was observed in the ^1H NMR spectrum thus suggesting that $ZnMe_2$ has a lower tendency to split the hafnium dimer than that of $AlMe_3$. In addition, no signs of reversible methyl exchange were detected in the ^1H EXSY NMR spectra. After 2 days at room temperature, the starting homobimetallic ion pair was consumed to give **1Me₂**, CH_4 and two new hafnium compounds (**a** and **b**) in approximately 1:1 ratio. The latter have three signals each: one signal for Cp resonances located at δ_H=5.54 and 5.21 ppm (δ_C=111.1 and 109.9 ppm), a singlet for Hf–CH_2 moieties at δ_H=0.13 and 1.85 ppm (δ_C=68.9 and 65.3 ppm) and a signal for Hf–CH_3 groups at δ_H= –0.35 and –0.42 ppm (δ_C=25.8 and 36.1 ppm); the relative signal intensities were 20:2:6 and 10:2:3 for **a** and **b**, respectively. By monitoring the composition of the reaction mixture as a function of time, it was observed that **a** formed initially to reach a steady state concentration, while the concentration of **b** increased as the starting ion pair decreased. ^1H NOE experiments showed the presence of rather strong dipolar contacts between Cp signals and both methyl and methylene resonances of the two species (Supporting Information). In addition, a NOE interaction was detected between methyl and methylene signals of **a** while, in the case of **b**, the interaction was notably weaker.

It is possible to hypothesize that the presence of **1Me$_2$** in the reaction mixture arose from the splitting of the starting bimetallic cation, while the formation of Hf-CH$_2$ moieties and the evolution of methane suggest that a σ-bond metathesis of Hf–Me groups occurred. By compiling all the pieces of information, it can be speculated that **a** corresponds to a bimetallic dimer featuring a CH$_2$ZnMe moiety, while **b** could be labeled as a monomeric [Cp$_2$Hf(CH$_2$ZnMe)][B(C$_6$F$_5$)$_4$] fragment. The ^{13}C chemical shift value of the methyl group in **b** suggests the presence of an interaction between the Zn–Me moiety and the Hf atom. An higher amount of **b** was obtained by using a larger amount of ZnMe$_2$ (20 equivalents), suggesting that it is likely formed from the breakage of the dimeric species **a**. No traces of dynamic processes were observed in the NOE spectrum, indicating that no reversible alkyl exchange occurs in the EXSY timescale.

c) Reactions with E(Et)$_n$. When **1(μ-Me)1** was mixed in toluene-d_8 with an excess of ZnEt$_2$ at 283K, ^{1}H NMR spectroscopy revealed the complete disappearance of the starting ion pair with the formation of **1Et$_2$** and other cationic products. The integration of the spectra indicated that all the methyl groups of the starting **1(μ-Me)1** were converted into ZnMe$_2$, suggesting a fast and irreversible ethyl transfer to hafnocene. The reaction mixture was unstable under these conditions and **1Et$_2$** was consumed in a further process where ethane and a new species formed. The ^{1}H NMR spectrum showed the presence of four Cp resonances (δ_H=5.23, 5.02, 4.94 and 4.79 ppm), an ABX spin system (three doublets of doublets at δ_H=3.43, 3.03 and 1.40 ppm, J$_{HH}$=17.0, 12.0 and 3.5 Hz) and a markedly shielded methyl group (δ_H= –2.13 ppm). The ABX spin system was identified as a –CH–CH$_2$ moiety by means of ^{1}H,^{13}C HSQC NMR spectrum and showed a δ_C=122.1 and δ_C=59.5 ppm for methyne and methylene moieties, respectively. The rather high chemical shift value of the CH moiety lead us to hypothesize the formation of a methyne-bridged bimetallic dimer, likely arising from a double σ-bond metathesis reaction of Hf-ethyl groups (Scheme 5). ^{1}H NOESY NMR experiments (Supporting Information) indicating the presence of selective dipolar interactions between the CHCH$_2$ moiety and the four magnetically non-equivalent cyclopentadienyl groups. The nature of methyl group located at δ_H=–2.13 ppm, having a ^{13}C chemical shift at δ_C=7.0 ppm, is unclear. Given that the latter showed strong NOE contacts only with the Cp rings, it can be speculated that it belongs to an anionic methylzincate fragment undergoing ion pairing with the bimetallic cation.
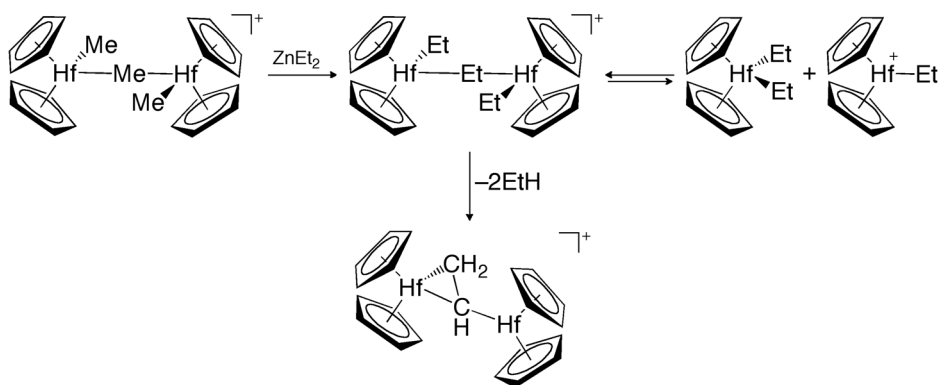
Scheme 5. Proposed reactivity of **1(μ-Me)1** with ZnEt$_2$.

When the reaction was performed with AlEt$_3$, a similar pathway was observed. At the end of the reaction, the ^{1}H NMR spectrum showed the presence of many products and two ABX spin systems (80:20 ratio) were observed. For the latter, ^{1}H and ^{13}C NMR chemical shift values were rather different to those obtained with ZnEt$_2$: the first pattern had δ_H=3.22, 0.70, 0.32 ppm and δ_C=70.5, 25.4 ppm while the second had δ_H=3.10, 0.94, 0.50 ppm and δ_C=69.8, 25.2 ppm. Assuming that the same bimetallic cation observed before formed, it can be inferred that the high low-frequency shift of the ^{13}C NMR resonances of the ABX spin system is due to bridging interactions with the excess of AlR$_3$ species.

Once again, no chemical exchange between any metallocene species and Al/Zn alkyls was observed, indicating that no reversible alkyl transfer occurs between hafnium and the main group metal and that σ-bond metathesis is the main active deactivation pathway. This seems to be in agreement with the general tendency of cationic hafnocenes to undergo bond methatesis with different substrates.[29]

5. Hafnium pyridylamido cationic species

Cationic species derived by the activation of **2Me$_2$** with [CPh$_3$][B(C$_6$F$_5$)$_4$] are known to undergo ligand exchange reactions with ZnR$_2$ or AlEt$_3$ at low temperature, affording heterobimetallic adducts in which the naphtyl group acts as a bridge between Hf and the main group metal.[16] To investigate the thermal transformation of such species, a sample of the heterobimetallic adduct with ZnMe$_2$ was synthesized in toluene-d_8 and kept at room temperature for 12 hours. The ^{1}H NMR spectrum of the solution obtained (Supporting Information) showed the presence of a prevalent set of sharp signals featuring typical fingerprints of pyridylamido hafnium complexes and a broad singlet at δ_H=0.73 ppm. The latter was assigned to BMe$_3$, reasonably arising from –C$_6$F$_5$ transfer reactions between ZnMe$_2$ and the anion.[28,30] In agreement, the ^{19}F NMR spectrum showed the disappearance of starting borate resonances with the formation of many sets of signals that were assigned to Zn(C$_6$F$_5$)$_2$ (δ_F=–118.4, –153.4 and –160.9 ppm)[30] and Hf–C$_6$F$_5$ moieties (*ortho* fluorine at δ_F=–119.4, –121.5, accounting for two F

atoms, and –125.5 ppm).[14b,31] The latter signals showed selective NOE interactions with pyridylamido protons in the ^{19}F,^1H HOESY NMR spectrum, thus confirming that two C_6F_5 rings are bound to the same hafnium atom. Therefore, the complete –C_6F_5 ring transfer to zinc and hafnium atoms (Scheme 6) led to the complete decomposition of borate anion and neutralization of pyridylamido cation. In perfect agreement with the latter hypothesis, a ^{13}C NMR signal at δ_C=209.3 ppm, showing long-range scalar correlations with naphthyl protons (Supporting Information), was observed thus confirming that the remetalation of the napthyl group occurred.

Interestingly, when **2Me₂** was activated with [HNMe₂Ph][B(C₆F₅)₄] to give the dimethyl cation featuring the demetalated naphthyl group[14b] and then reacted with ZnMe₂, no reaction took place at room temperature and B(C₆F₅)₄⁻ did not decompose. Reversible methyl transfer between Zn and Hf atoms was shown to occur, but the superimposed methyl groups hampered the quantification of the rate constants by ^1H EXSY NMR spectroscopy.
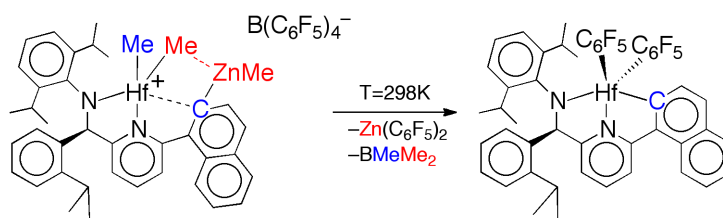
Scheme 6. Thermal evolution of pyridylamidoHfMe/ZnMe₂ adducts.

In the case of the adduct with AlMe₃, the thermal transformation at room temperature was more complex and led to the formation of two prevalent species in a 1:1 ratio, as deduced by the presence of 6 septets due to isopropyl groups in the ^1H NMR spectrum. The ^{19}F NMR spectrum showed the appearance of both Al– and Hf–C₆F₅ moieties that, together with the presence of BMe₃ in the ^1H NMR spectrum, confirmed borate anion decomposition. Different to what was observed with ZnMe₂, an accurate analysis of the long range interactions in the ^1H,^{13}C HMQC spectrum revealed that no remetalation of the naphthyl occurred. The first product showed two doublets located at δ_H=4.60 and 0.98 ppm ($^3J_{HH}$=7.8 Hz, δ_C=74.1 ppm) and a Al–Me group falling at δ_H=–0.88 ppm. A ^{19}F,^1H HOESY NMR spectrum showed that such resonances had selective NOE interactions with one *ortho*-F atom belonging to a Hf–C₆F₅. The second product showed the presence of an Hf–Me group at δ_H=1.72 ppm (δ_C=69.5 ppm) that was dipolarly coupled with another *ortho*-F of an Hf-C₆F₅ moiety. Full characterization of the complex was hampered by the overlapping of many signals but it was possibile to conclude that aluminium has no tendency to detach from the naphthyl group, opening the route for new deactivation pathways including the formation of bridging Hf-CH₂-Al moieties arising from σ-bond metathesis.

6. Conclusions

The reactions of organometallic Hf(IV) complexes with ZnR$_2$ and AlEt$_3$ (R= Me or Et) have been explored by means of NMR spectroscopy, with the main purpose of obtaining insights into alkyl transfer processes that are central to coordinative chain transfer olefin polymerization catalysis. The simplest hafnocene **1Me$_2$** and highly-optimized pyridylamido **2Me$_2$** have been chosen as a case study, in order to contrast a poorly performing metallocene and an industrially relevant post-metallocene featuring the same transition metal. The main conclusion of this work is that the efficiency of the chain transfer is not arising from the nature of the single transition or main group metal complex, but reflects the matching between them. The investigation of the reactivity of neutral dimethyl species with ER$_n$ revealed that the ancillary ligand plays a remarkable role in determining both rate and reversibility of alkyl exchange between hafnium and main metal. In fact, metallocene reacts slowly with both ZnEt$_2$ and AlEt$_3$ to give methyl to ethyl exchange, while postmetallocene reacts much faster and reversibly. Variable temperature kinetic studies relate this difference to the notably lower activation enthalpy of the reaction with **2Et$_2$** ($\Delta\Delta H^{\neq}$=8 kcal/mol with ZnEt$_2$) whereas activation entropy values have shown to be large and negative in all the cases, pointing to an associative reaction mechanism. The nature of chain transfer agent was found to be important only in the case of metallocene ethylation, where the alkyl transfer occurs out of the equilibrium. In this case, AlEt$_3$ reacts faster than ZnEt$_2$ due to a lower $\Delta H^{\neq}$ value. On the contrary, pyridylamido precatalysts undergo fast and reversible alkyl exchange with both Al– and Zn– alkyls with comparable activation barriers, reasonably due to the combination of higher Lewis acidity and less steric encumbrance at the metal centre in postmetallocene framework.

As far as cationic species are concerned, homobimetallic **1(μ-Me)1** ion pair reacts with ER$_n$ affording different products whose structure depends on the nature of both E and R. In the case of AlMe$_3$, the bimetallic cation is readily split into **1Me$_2$** and heterobimetallic **1(μ-Me)Al** ion pair, which have been found to undergo slow selective chemical exchange formally due to [AlMe$_2$][B(C$_6$F$_5$)$_4$] ion pairs transfer. ZnMe$_2$ is instead less electrophilic and does not favor the cleavage of the bimetallic cation. However, it stimulates a very slow σ-bond metathesis reaction leading to the formation of methane and Hf-CH$_2$-Zn moieties. In the case of ZnEt$_2$ and AlEt$_3$, a fast irreversible ethylation of the bimetallic cation occurs but, even at low temperature, rapid metathesis reactions affording ethane and methyne-bridged bimetallic cations take place. Interestingly, none of the formed species exhibit reversible chemical exchange with ER$_n$, indicating that this kind of process is still difficult for cationic hafnocenes. Heterobimetallic [pyridylamido(Hf)Me(μ-Me)EMe$_{n-1}$][B(C$_6$F$_5$)$_4$] adducts showed rapid decomposition of the borate anion to BMe$_3$ as main deactivation pathway. Interestingly, remetalation of the naphthyl group on the Hf atom was observed when E=Zn. This strongly supports that the formation of heterobimetallic adducts with Zn is a reversible reaction, as previously suggested.[16] In the case of the adduct with Al, no remetalation occurs and other decomposition pathways take place leading to the formation of Al–CH$_2$–Hf moieties.

7. Experimental Section

Materials and methods. All manipulations of air-sensitive materials were performed in flamed Schlenk glassware on a Schlenk line, interfaced to a high-vacuum pump (10^{-5} mmHg), or in a nitrogen-filled Vac-Atmosphere glovebox with a high capacity recirculator (<1 ppm O_2 and H_2O). All solvents were preventively distilled after 12 h reflux over Na and freeze-pump-thaw degassed over Na/K alloy. Benzene-d_6 and toluene-d_8 were freeze-pump-thaw degassed over Na/K alloy, vacuum transferred into a Schlenk flask with a PTFE valve and stored over activated molecular sieves.

Bis-cyclopentadienyl-hafnium-dimethyl (**1Me$_2$**) was purchased from Strem Chemicals and used as received. [N-[2,6-Diisopropylphenyl]-α-[2-isopropylphenyl]-6-(1-naphthalenyl)-2-pyridinemethanaminato]hafnium dimethyl (**2Me$_2$**) was obtained as a gift from Dow Chemical and was used as received. [CPh$_3$][B(C$_6$F$_5$)$_4$] was obtained from Boulder Scientific and used as received. ZnMe$_2$ (2.0 M solution in toluene), ZnEt$_2$ (Zn 52% wt.), AlMe$_3$ (97%) and AlEt$_3$ (93%) were purchased from Sigma Aldrich and used as received. *CAUTION: tri-alkylaluminum and dialkyl-zinc are pyrophoric and must be handled in rigorously dry conditions.*

^{1}H, ^{1}H inversion recovery, ^{13}C{^{1}H}, ^{1}H COSY, ^{1}H NOESY, ^{1}H EXSY, ^{1}H,^{13}C HMQC, ^{1}H,^{13}C HSQC, ^{1}H,^{13}C HMBC, ^{19}F and ^{19}F,^{1}H HOESY NMR experiments were performed on a Bruker Avance DRX 400 equipped with a QNP probe or on a Bruker Avance III 400 equipped with a ^{1}H, BB smartprobe. Referencing by residual solvents is relative to TMS. The actual concentration of the samples was estimated from integration relative to an external standard.

In *situ* reactions and NMR data. Dimethyl precursors/ER$_n$ mixtures were generated within the glovebox, by dissolving the suitable amount of **1Me$_2$** or **2Me$_2$** in approximately 0.7 ml of benzene-d_6 or toluene-d_8 and by injecting the required volume of ZnR$_2$ or AlEt$_3$ with a micrometric syringe. Immediately after mixing, the tube was sealed, transferred out of the glovebox and inserted into a cold bath. **1(μ−Me)1** was synthesized *in situ*, by loading the suitable amount of **1Me$_2$** and 0.5 equivalents of [CPh$_3$][B(C$_6$F$_5$)$_4$] into a J Young NMR tube and adding approximately 0.7 ml of toluene-d_8. Further reactions of **1(μ−Me)1** with ER$_n$ were performed as described above. **2(C$_6$F$_5$)$_2$** was obtained by activating **2Me$_2$** with 1.0 equivalents of [CPh$_3$][B(C$_6$F$_5$)$_4$] in toluene-d_8 and by reacting the formed ion pair with 5 equivalents of ZnMe$_2$ at room temperature.

Cp$_2$HfMe$_2$ (**1Me$_2$**). ^{1}H NMR (400 MHz, benzene-d_6, 298K): δ=5.65 (s, Cp), –0.33 ppm (s, Me). ^{13}C{^{1}H} NMR (100.55 MHz, benzene-d_6, 298K): δ=110.0 (s, Cp), 36.4 ppm (s, Me).

Cp$_2$HfMeEt (**1MeEt**). ^{1}H NMR (400 MHz, benzene-d_6, 298K): δ=5.65 (s, Cp), 1.41 (t, ^{3}J$_{HH}$=7.7 Hz, CH$_2$*Me*), 0.89 (q, ^{3}J$_{HH}$=7.7 Hz, C*H$_2$*Me), –0.40 ppm (s, Me). ^{13}C{^{1}H} NMR (100.55 MHz, benzene-d_6, 298K): δ=110.0 (s, Cp), 49.0 (s, *CH$_2$*Me), 36.6 (s, Me), 16.0 (s, CH$_2$*Me*).

Cp$_2$HfEt$_2$ (**1Et$_2$**). ^{1}H NMR (400 MHz, benzene-d_6, 298K): δ=5.66 (s, Cp), 1.43 (t, ^{3}J$_{HH}$=7.8 Hz, CH$_2$*Me*), 0.89 ppm (q, ^{3}J$_{HH}$=7.8 Hz, C*H$_2$*Me). ^{13}C{^{1}H} NMR (100.55 MHz, benzene-d_6, 298K): δ=110.0 (s, Cp), 49.1 (s, *CH$_2$*Me), 16.1 (s, CH$_2$*Me*).

[(Cp$_2$HfMe)$_2$(μ–Me)][B(C$_6$F$_5$)$_4$] (**1(μ–Me)1**). ^{1}H NMR (400 MHz, toluene-d_8, 298K): δ=5.51 (s, Cp), –0.32 (s, HfMe), –1.21 ppm (s, Hf(μ-Me)). ^{13}C{^{1}H} NMR (400 MHz, toluene-d_8, 298K): δ=111.7 (s, Cp), 40.0 (s, HfMe), 22.6 ppm (s, Hf(μ-Me)). ^{19}F NMR (376.65 MHz, toluene-d_8, 298K): δ=–131.8 (brd, *o*-F B(C$_6$F$_5$)$_4$), –162.1 (t, $^3J_{FF}$= 20.8 Hz, *p*-F B(C$_6$F$_5$)$_4$), –166.1 ppm (m, *m*-F B(C$_6$F$_5$)$_4$).

[Cp$_2$Hf(μ–Me)$_2$AlMe$_2$][B(C$_6$F$_5$)$_4$] (**1(μ–Me)Al**). ^{1}H NMR (400 MHz, toluene-d_8, 298K): δ=5.37 (s, Cp), –0.07 (s, HfMe), –0.75 ppm (s, AlMe). ^{13}C{^{1}H} NMR (400 MHz, toluene-d_8, 298K): δ=113.4 (s, Cp), 36.0 (s, HfMe), –7.05 ppm (s, AlMe). ^{19}F NMR (376.65 MHz, toluene-d_8, 298K): δ=–131.8 (brd, *o*-F B(C$_6$F$_5$)$_4$), –162.1 (t, $^3J_{FF}$= 20.8 Hz, *p*-F B(C$_6$F$_5$)$_4$), –166.1 ppm (m, *m*-F B(C$_6$F$_5$)$_4$).

1(μ–Me)1+ ZnMe$_2$. ^{1}H NMR (400 MHz, toluene-d_8, 298K): δ=5.54 (s, Cp (**a**)), 5.21 (s, Cp (**b**)), 1.85 (s, CH$_2$ (**b**)), 0.13 (s, CH$_2$ (**a**)), –0.35 (s, Me (**a**)), –0.42 ppm (s, Me (**b**)). ^{13}C{^{1}H} NMR (400 MHz, toluene-d_8, 298K): δ=111.1 (s, Cp (**a**)), 109.9 (s, Cp (**b**)), 68.9 (s, CH$_2$ (**a**)), 65.3 (s, CH$_2$ (**b**)), 36.1 (s, Me (**a**)), 25.8 ppm (s, Me (**b**)). ^{19}F NMR (376.65 MHz, toluene-d_8, 298K): δ=–131.5 (brd, *o*-F B(C$_6$F$_5$)$_4$), –162.1 (t, $^3J_{FF}$= 20.8 Hz, *p*-F B(C$_6$F$_5$)$_4$), –165.9 ppm (m, *m*-F B(C$_6$F$_5$)$_4$).

1(μ–Me)1+ ZnEt$_2$. Selected ^{1}H NMR resonances (400 MHz, toluene-d_8, 298K): δ=5.23 (s, H4), 5.02 (s, H2), 4.94 (s, H3), 4.79 (s, H1), 3.43 (dd, $^3J_{HH}$=16.4, 12.0 Hz, H6), 3.03 (dd, $^3J_{HH}$=12.0 $^2J_{HH}$=3.3 Hz, H5a), 1.40 ppm (overlapped with **1Et$_2$**, H5b). Selected ^{13}C{^{1}H} NMR resonances (100.55 MHz, toluene-d_8, 298K): δ=122.2 (s, C6), 107.2 (s, C4), 105.9 (s, C2), 105.7 (s, C3), 105.1 (s, C1), 59.5 ppm (s, C5). ^{19}F NMR (376.65 MHz, toluene-d_8, 298K): δ=–131.6 (brd, *o*-F B(C$_6$F$_5$)$_4$), –162.2 (t, $^3J_{HH}$= 20.8 Hz, *p*-F B(C$_6$F$_5$)$_4$), –166.1 ppm (m, *m*-F B(C$_6$F$_5$)$_4$).
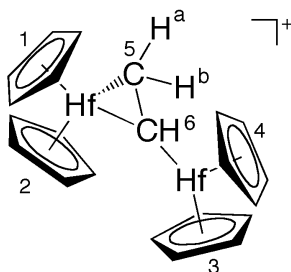
1(μ–Me)1+ AlEt$_3$. Selected ^{1}H NMR resonances (400 MHz, toluene-d_8, 298K): δ=5.87 (s, Cp), 5.36 (s, Cp), 5.46 (s, Cp), 5.84 (s, Cp), 3.07 (dd, $^3J_{HH}$=17.2, 11.2 Hz, CH), 0.89 (m, CH$_2$), 0.43 ppm (m, CH$_2$). Selected ^{13}C{^{1}H} NMR resonances (100.55 MHz, toluene-d_8, 298K): δ=114.3 (s, Cp), 113.5 (s, Cp), 105.1 (s, Cp), 104.6 (s, Cp), 69.8 (s, CH), 25.2 ppm (s, CH$_2$).

[N-[2,6-Diisopropylphenyl]-α-[2-isopropylphenyl]-6-(1-naphthalenyl)-2-pyridinemethanami–nato]hafnium dimethyl (**2Me$_2$**). ^{1}H NMR (400 MHz, benzene-d_6, 298K): δ=8.58 (d, $^3J_{HH}$=7.7 Hz, H2), 8.25 (d, $^3J_{HH}$=8.6 Hz, H8), 7.82 (d, $^3J_{HH}$=7.7 Hz, H3), 7.72 (dd, $^3J_{HH}$=7.6, $^4J_{HH}$=2.0 Hz, H5), 7.50 (d, $^3J_{HH}$=8.0 Hz, H12), 7.34 (m, H24), 7.29 (m, H6+H7), 7.15 (m, H30+H31), 7.07 (m, H21+H29), 7.00 (m, H22+H23), 6.82 (t, $^3J_{HH}$=8.0 Hz, H13), 6.57 (s, H16), 6.55 (d, $^3J_{HH}$=8.0 Hz, H14), 3.83 (sept, $^3J_{HH}$=6.8 Hz, H27), 3.37 (sept, $^3J_{HH}$=6.8 Hz, H33), 2.89 (sept, $^3J_{HH}$=6.9 Hz, H19), 1.38 (d, $^3J_{HH}$=6.8 Hz,

H34'), 1.37 (d, $^3J_{HH}$=6.8 Hz, H28), 1.18 (d, $^3J_{HH}$=6.8 Hz, H20), 1.14 (d, $^3J_{HH}$=6.8 Hz, H34), 0.96 (s, H35), 0.70 (s, H36), 0.69 (d, $^3J_{HH}$=6.8 Hz, H20'), 0.39 ppm (d, $^3J_{HH}$=6.8 Hz, H28'). ^{13}C{^{1}H} NMR (100.55 MHz, benzene-d_6, 298K): δ=171.2 (s, C15), 165.0 (s, C11), 148.0 (s, C26), 147.4 (s, C18), 147.0 (s, C32), 146.2 (s, C25), 144.7 (s, C10), 141.5 (s, C17), 141.4 (s, C13), 136.4 (s, C9), 134.8 (s, C2), 131.4 (s, C4), 130.8 (s, C24), 130.6 (s, C5), 130.5 (s, C3), 128.5 (s, overlapped with C_6D_6, C22), 127.6 (s, C6 or C7), 127.4 (s, C23), 126.7 (s, C30), 126.2 (s, C7 or C6), 126.1 (s, C21), 125.8 (s, C31), 125.2 (s, C29), 124.9 (s, C8), 121.1 (s, C12), 120.2 (s, C14), 77.4 (s, C16), 67.6 (s, C36), 63.5 (s, C35), 29.4 (s, C33), 29.3 (s, C19), 28.8 (s, C27), 28.1 (s, C28), 26.5 (s, C34'), 26.1 (s, C34), 25.8 (s, C20), 24.4 (s, C28'), 23.7 ppm (s, C20').
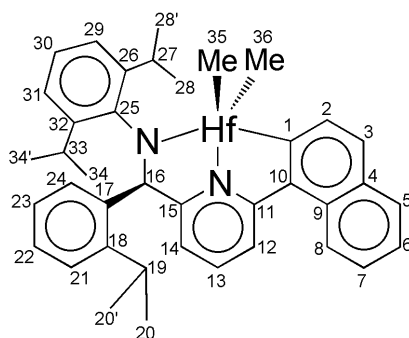
syn/*anti* [N-[2,6-Diisopropylphenyl]-α-[2-isopropylphenyl]-6-(1-naphthalenyl)-2-pyridineme–thanaminato]hafnium methyl-ethyl (**2MeEt**). Selected ^{1}H NMR resonances (400 MHz, benzene-d_6, 298K): δ=8.66 (d, $^3J_{HH}$=7.7 Hz, H2 syn or anti), 8.65 (d, $^3J_{HH}$=7.7 Hz, H2 syn or anti), 8.26 (d, overlapped with HfEt$_2$, H8 syn+anti) 7.81 (d, $^3J_{HH}$=7.7 Hz, H3 syn+anti), 7.72 (d, overlapped with HfEt$_2$, H5 syn+anti), 7.52 (d, overlapped with HfEt$_2$, H12 syn+anti), 7.35 (m, overlapped with HfEt$_2$, H24 syn+anti), 7.29 (m, overlapped with HfEt$_2$, H6+H7 syn+anti), 6.85 (t, overlapped with HfEt$_2$, H13 syn+anti), 6.57 (s, overlapped with HfEt$_2$, H16 syn+anti), 6.55 (d, overlapped with HfEt$_2$, H14 syn+anti), 3.75 (sept, overlapped with HfEt$_2$, H27 syn+anti), 3.37 (sept, overlapped with HfEt$_2$, H33 syn+anti), 2.89 (sept, overlapped with HfEt$_2$, H19 syn+anti), 1.75 (t, $^3J_{HH}$=8.0 Hz, H36 syn), 1.53 (t, $^3J_{HH}$=8.0 Hz, H37 anti), 1.50 (m, H35 syn), 1.39 (overlapped with HfEt$_2$, H34'+H28 syn+anti), 1.28 (overlapped with HfEt$_2$, H36 anti + H20+H34 syn+anti), 1.05 (m, overlapped with HfEt$_2$, H35 syn), 1.04 (s, H35 anti), 0.84 (m, overlapped with HfEt$_2$, H36 anti), 0.70 (m, overlapped with HfEt$_2$, H37 syn+H20'syn+anti), 0.36 ppm (overlapped with HfEt$_2$, H28' syn+anti).
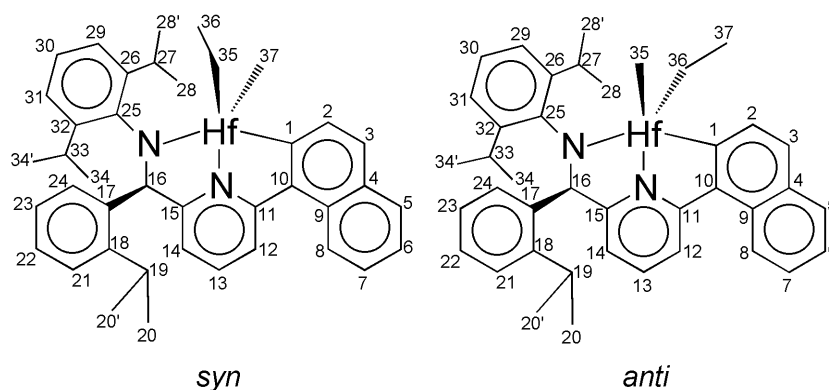
syn   *anti*

[N-[2,6-Diisopropylphenyl]-α-[2-isopropylphenyl]-6-(1-naphthalenyl)-2-pyridinemethanami–nato]hafnium diethyl (**2Et₂**). ^{1}H NMR (400 MHz, toluene-d_8, 298K): δ=8.62 (d, $^3J_{HH}$=7.7 Hz, H2), 8.20 (d, $^3J_{HH}$=8.2 Hz, H8), 7.76 (d, $^3J_{HH}$=7.7 Hz, H3), 7.68 (dd, $^3J_{HH}$=7.4, $^4J_{HH}$=2.0 Hz, H5), 7.50 (d, $^3J_{HH}$=8.0 Hz, H12), 7.30 (m, H24), 7.26 (m, H6+H7), 7.13 (dd, $^3J_{HH}$=7.4 and 1.9 Hz, H31), 7.07-7.00 (m, H29+H30+H21+H22+H23), 6.91 (t, $^3J_{HH}$=7.8 Hz, H13), 6.60 (d, $^3J_{HH}$=7.8 Hz, H14), 6.54 (s, H16), 3.68 (sept, $^3J_{HH}$=6.8 Hz, H27), 3.68 (sept, $^3J_{HH}$=6.8 Hz, H27), 3.34 (sept, $^3J_{HH}$=6.8 Hz, H33), 2.87 (sept, $^3J_{HH}$=6.8 Hz, H19), 1.72 (t, $^3J_{HH}$=8.0 Hz, H36), 1.44 (m, H38+H35b), 1.39 (d, $^3J_{HH}$=6.8 Hz, H34'), 1.34 (d, $^3J_{HH}$=6.8 Hz, H28), 1.18 (d, $^3J_{HH}$=6.8 Hz, H20), 1.15 (d, $^3J_{HH}$=6.8 Hz, H34), 1.08 (m, H35a), 0.98 (m, H37b), 0.76 (m, H37a), 0.66 (d, $^3J_{HH}$=6.8 Hz, H20'), 0.30 ppm (d, $^3J_{HH}$=6.8 Hz, H28'). ^{13}C{^{1}H} NMR (100.55 MHz, toluene-d_8, 298K): δ=205.0 (s, C1), 170.3 (s, C15), 164.1 (s, C11), 147.2 (s, C26), 146.5 (s, C18), 146.1 (s, C32), 145.9 (s, C25), 144.0 (s, C10), 141.1 (s, C17), 140.3 (s, C13), 135.4 (s, C9), 134.2 (s, C2), 130.5 (s, C4), 130.1 (s, C24), 129.6 (s, C5), 129.5 (s, C3), 127.5 (s, overlapped with C_7D_8, C22), 126.6 (s, C6 or C7), 126.5 (s, C23), 125.6 (s, C30), 125.2 (s, C21 or C29), 125.0 (s, overlapped with C_7D_8, C7 or C6), 124.8 (s, C31), 124.3 (s, C29 or C21), 123.9 (s, C8), 120.2 (s, C12), 119.1 (s, C14), 79.2 (s, C37), 76.6 (s, C16), 74.7 (s, C35), 28.5 (s, C19), 28.4 (s, C33), 28.0 (s, C27), 26.9 (s, C28), 25.9 (s, C34'), 25.2 (s, C34), 25.0 (s, C20), 23.7 (s, C28'), 22.8 (s, C20'), 11.7 (s, C38), 11.3 ppm (s, C36).
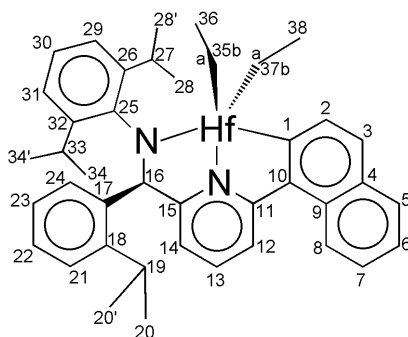

[N-[2,6-Diisopropylphenyl]-α-[2-isopropylphenyl]-6-(1-naphthalenyl)-2-pyridinemethanami–nato]hafnium bis-perfluorophenyl (**2(C₆F₅)₂**). Selected ^{1}H NMR resonances (400 MHz, toluene-d_8, 298K): δ=8.17 (d, $^3J_{HH}$=8.7 Hz, H8), 8.01 (d, $^3J_{HH}$=7.9 Hz, H2), 7.54 (d, H3+H5+H24), 7.48 (m,

H6+H12), 7.16 (m, H7), 6.87 (m, overlapped with other aromatic resonances, H13), 6.75 (s, H16), 6.53 (d, $^3J_{HH}$=7.8 Hz, H14), 3.25 (sept, $^3J_{HH}$=6.8 Hz, H27), 3.03 (sept, $^3J_{HH}$=6.8 Hz, H33), 2.53 (sept, $^3J_{HH}$=6.8 Hz, H19), 1.26 (d, $^3J_{HH}$=6.8 Hz, H34'), 1.07 (d, $^3J_{HH}$=6.8 Hz, H20), 0.61 (d, $^3J_{HH}$=6.8 Hz, H28), 0.56 (d, $^3J_{HH}$=6.8 Hz, H20'), 0.24 (d, $^3J_{HH}$=6.8 Hz, H34), –0.03 ppm (d, $^3J_{HH}$=6.8 Hz, H28'). Selected $^{13}C\{^1H\}$ NMR resonances (100.55 MHz, toluene-d_8, 298K): δ=209.5 (s, C1), 171.9 (s, C15), 165.4 (s, C11), 148.6 (s, C26), 147.8 (s, C18), 146.5 (s, C32), 143.0 (s, C10), 142.4 (s, C13), 130.7 (s, C3), 130.2 (s, C2), 124.1 (s, C8), 120.8 (s, C14), 120.4 (s, C12), 77.4 (s, C16), 29.0 (s, C33), 28.5 (s, C19), 28.3 (s, C27), 26.7 (s, C34'), 25.9 (s, C20), 25.0 (s, C28), 23.9 (s, C28'), 23.7 (s, C34), 22.0 ppm (s, C20'). ^{19}F NMR (376.65 MHz, toluene-d_8, 298K): δ= –119.4 (brd, o–F –C_6F_5), –121.4 (brd, o–F –C_6F_5), –125.5 (brd, o–F –C_6F_5), –151.3 (t, $^3J_{FF}$=19.4 Hz, p–F –C_6F_5), –151.9 (t, $^3J_{FF}$=19.4 Hz, p–F –C_6F_5), –160.9 (m, m–F –C_6F_5), –161.5 ppm (m, m–F –C_6F_5).
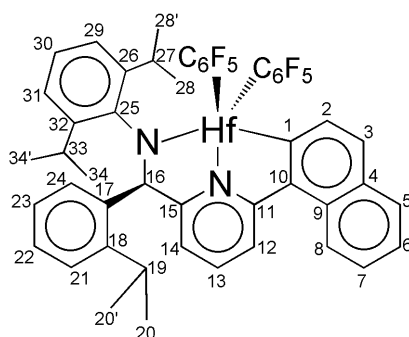
Kinetic measurements. Slow ethylation reactions were performed in J–Young tubes containing cold mixtures of **1Me₂** and alkylating agent, which were inserted into the NMR probe and allowed to equilibrate at the desired instrumental temperature. The composition of the reaction mixture was monitored by means of ^1H NMR spectroscopy by acquiring a series of spectra as a function of time. Concentration *versus* time plots were obtained by referencing to an external standard and fitted by means of COPASI software package.[32] The reaction plots were interpolated with a two-reactions kinetic model of the type:

$$Cp_2HfMe_2 + E(Et) \xrightarrow{k_1} Cp_2HfMeEt + E(Me)$$

$$Cp_2HfMeEt + E(Et) \xrightarrow{k_2} Cp_2HfEt_2 + E(Me)$$
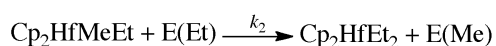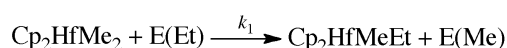
where E(Et) and E(Me) are the total concentration of ethyl and methyl groups bound to Al or Zn atoms. Due to the presence of a large excess of alkylating agent, equilibrium effects were neglected. At higher temperatures, a decomposition reaction was added to the kinetic model to take into account the formation of ethane and improve the quality of the fitting.

Fast and reversible exchange rates between **2Et₂** and E(Et)$_n$ were quantified by means of two-dimensional ^1H EXSY NMR spectroscopy, by using the *pfg* version of the standard ^1H NOESY se-

quence (noesygptp). Different values of spectral width, relaxation delay, mixing time (τ_M) and number of transients were used according to the sample nature and concentration. Microscopic rate constants (k', s^{-1}) were calculated from the integration of the 2D spectra by using the software EXSYCALC[33] and converted into second order rate constants (k, M^{-1} s^{-1}) correcting by the actual molar concentration of the exchanging sites. At least two experiments with different τ_M values were acquired and the rate constant values (with relative standard deviations) were obtained from the average of all the values.
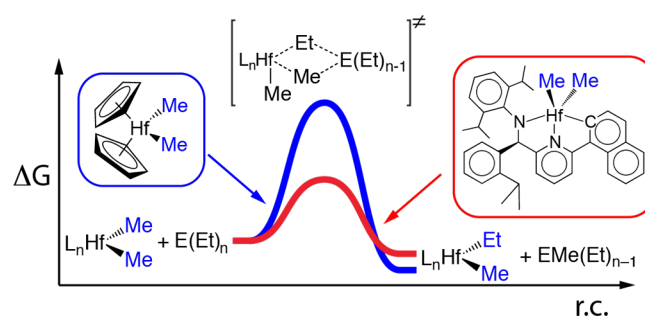
T1 values for the exchanging resonances were measured by means of ^{1}H inversion recovery experiments and, in all cases, no differences in T1 were observed.

For the Table of Contents:

References

1) (a) Amin, S. B.; Marks, T. J. *Angew. Chem. Int. Ed.* **2008**, *47*, 2006–2025. (b) Makio, H.; Ochiai, T.; Mohri, J.; Takeda, K.; Shimazaki, T.; Usui, Y.; Matsuura, S.; Fujita, T. *J. Am. Chem. Soc.* **2013**, *135*, 8177–8180.

2) (a) Klimpel, M. G.; Eppinger, J.; Sirsch, P.; Scherer, W.; Anwander, R. *Organometallics* **2002**, *21*, 4021–4023. (b) Busico, V.; Cipullo, R.; Cutillo, F.; Friederichs, N.; Wang, B. *J. Am. Chem. Soc.* **2003**, *125*, 12402–12403. (c) Fan, G.; Dong, J. Y. *J. Mol. Catal. A: Chem.* **2005**, *236*, 246–252. (d) Bhriain, N. N.; Brintzinger, H. H.; Ruchatz, D.; Fink, G. *Macromolecules* **2005**, *38*, 2056–2063. (e) Quintanilla, E.; di Lena, F.; Chen, P. *Chem. Commun.* **2006**, 4309–4311.

3) Zijlstra, H. S.; Harder, S. *Eur. J. Inorg. Chem.* **2015**, 19–43.

4) (a) Lieber, S.; Brintzinger, H. H. *Macromolecules* **2000**, *33*, 9192–9199. (b) Bogaert, S.; Chenal, T.; Mortreux, A.; Carpentier, J. F *J. Mol. Catal. A: Chem.* **2002**, *190*, 207–214. (c) Tynys, A.; Saarinen, T.; Hakala, K.; Helaja, T.; Vanne, T.; Lehmus, P.; Löfgren, B. *Macromol. Chem. Phys.* **2005**, *206*, 1043–1056. (d) Busico, V.; Cipullo, R.; Pellecchia, R.; Talarico, G.; Razavi, A. *Macromolecules* **2009**, *42*, 1789–1791. (e) Rouholahnejad, F.; Mathis, D.; Chen. P. *Organometallics* **2010**, *29*, 294–302. (f) Camara, J. M.; Petros, R. A.; Norton, J. R. *J. Am. Chem. Soc.* **2011**, *133*, 5263–5273.

5) (a) Coates, G. W.; Hustad, P. D.; Reinartz, S. *Angew. Chem. Int. Ed* **2002**, *41*, 2236–2257. (b) Domski, G. J.; Rose, J. M.; Coates, G. W.; Bolig, A. D.; Brookhart, M. *Prog. Polym. Sci.* **2007**, *32*, 30–92.

6) Sita, L. *Angew. Chem. Int. Ed.* **2009**, *48*, 2464–2472.

7) General references on CCTP: (a) Van Meurs, M.; Britovsek, G. J. P.; Gibson, V. C.; Cohen, S. A. *J. Am. Chem. Soc.* **2005**, *127*, 9913–9923. (b) Kempe, R. *Chem. Eur. J.* **2007**, *13*, 2764–2773. (c) Valente, A.; Mortreux, A.; Visseaux, M.; Zinck, P. *Chem. Rev.* **2013**, *113*, 3836–3857. (d) Ribeiro, R.; Ruivo, R.; Nsiri, H.; Norsic, S.; D'Agosto, F.; Perrin, L.; Boisson, C. *ACS Catal.* **2016**, *6*, 851–860.

8) (a) Hustad, P. D.; Kuhlman, R. L.; Arriola, D. J.; Carnahan, E. M.; Wenzel, T. T. *Macromolecules* **2007**, *40*, 7061–7064. (b) Zhang, W.; Sita, L. R. *J. Am. Chem. Soc.* **2008**, *130*, 442–443.

9) (a) Bochmann, M.; Lancaster, S. J. *Angew. Chem. Int. Ed.* **1994**, *33*, 1634–1637. (b) Bochmann, M.; Lancaster, S. J. *J. Organomet. Chem.* **1995**, *497*, 55–59. (c) Götz, C.; Rau, A.; Luft, G. *J. Mol. Catal. A: Chem.* **2002**, *184*, 95–110. (d) Bryliakov, K. P.; Semikolenova, N. V.; Yudaev, D. V.; Zakharov, V. A.; Brintzinger, H. H., Ystenes, M.; Rytter, E.; Talsi, E. P.; *J. Organomet. Chem.* **2003**, *683*, 92–102. (e) Bryliakov, K. P.; Talsi, E. P.; Voskoboynikov, A. Z.; Lancaster, S. J.; Bochmann, M. *Organometallics* **2008**, *27*, 6333–6342. (f) Mathis, D.; Couzijn, E. P. A.; Chen, P. *Organometallics* **2011**, *30*, 3834–3843. (g) Rocchigiani, L.; Busico, V.; Pastore A.; Macchioni, A. *Dalton Trans.* **2013**, *42*, 9104–9111.

10) Dettenrieder, N.; Hollfelder, C. O.; Jende, L. N.; Maichle-Mössmer, C.; Anwander, R. *Organometallics* **2014**, *33*, 1528–1531.

11) Soshnikov, I. E.; Semikolenova, N. V.; Antonov, A. A.; Bryliakov, K. P.; Zakharov, V. A.; Talsi, E. P. *Organometallics* **2014**, *33*, 2583–2587.

12) Bryliakov, K. P.; Semikolenova, N. V.; Zakharov, V. A.; Talsi, E. P. *Organometallics* **2004**, *23*, 5375–5378.

13) Soshnikov, I. E.; Semikolenova, N. V.; Bushmelev, A. N.; Bryliakov, K. P.; Lyakin, O. Y.; Redshaw, C.; Zakharov, V. A.; Talsi, E. P. *Organometallics* **2009**, *28*, 6003–6013.

14) (a) Boussie, T. R.; Diamond, G. M.; Goh, C.; Hall, K. A.; LaPointe, A. M.; Leclerc, M. K.; Lund, C.; Murphy, V.; Shoemaker, J. A. W.; Turner, H.; Rosen, R. K.; Stevens, J. C.; Alfano, F.; Busico, V.; Cipullo, R.; Talarico, G. *Angew. Chem. Int. Ed.* **2006**, *45*, 3278–3283. (b) Zuccaccia, C.; Macchioni, A.; Busico, V.; Cipullo, R.; Talarico, G.; Alfano, F.; Boone, H. W.; Frazier, K. A.; Hustad, P. D.; Stevens, J. C.; Vosejpka, P. C.; Abboud, K. A. *J. Am. Chem. Soc.* **2008**, *130*, 10354–10368. (c) Zuccaccia, C.; Busico, V.; Cipullo, R.; Talarico, G.; Froese, R. D. J.; Vosejpka, P. C.; Hustad, P. D.; Macchioni, A. *Organometallics* **2009**, *28*, 5445–5458. (d) Li, G.; Zuccaccia, C.; Tedesco, C.; D'Auria, I.; Macchioni, A.; Pellecchia, C. *Chem. Eur. J.* **2014**, *20*, 232–244.

15) (a) Arriola, D. J.; Carnahan, E. M.; Hustad, P. D.; Kuhlman, R. L.; Wenzel, T. T. *Science* **2006**, *312*, 714–719. (b) Hustad, P. D.; Kuhlman, R. L.; Carnahan, E. M.; Wenzel, T. T.; Arriola, D. J. *Macromolecules* **2008**, *41*, 4081–4089.

16) Rocchigiani, L.; Busico, V.; Pastore, A.; Talarico, G.; Macchioni, A. *Angew. Chem. Int. Ed.* **2014**, *53*, 2157–2161.

17) (a) Liu, Z; Somsook, E.; White, C.B.; Rosaaen, K. A.; Landis, C. R. *J. Am. Chem. Soc.* **2001**, *123*, 11193–11207. (b) Christianson, M. D.; E. H. P. Tan, Landis, C. R. *J. Am. Chem. Soc.* **2010**, 132, 11461–11463. (c) Rocchigiani, L.; Ciancaleoni, G.; Zuccaccia, C.; Macchioni, A. *Angew. Chem. Int. Ed.* **2011**, *50*, 11752–11755. (d) Rocchigiani, L.; Macchioni, A. *Dalton Trans.* **2016**, *45*, 2785–2790.

18) (a) Brown, T. L.; Murrell, L. L. *J. Am. Chem. Soc.* **1972**, *94*, 378–384. (b) Jeffery, E. A.; Mole, T. *Aust. J. Chem.* **1973**, *26*, 739–748.

19) Williams, K. C.; Brown, T. L. *J. Am. Chem. Soc.* **1966**, *88*, 5460–5465.

20) At the coalescence temperature, $k = \dfrac{\pi \Delta v_0}{\sqrt{2}}$ (Δv_0 is the distance in Hz between the signals in the completely resolved spectrum).

21) Siedle, A. R.; Newmark, R. A.; Schroepfer, J. N.; Lyon. P A. *Organometallics* **1991**, *10*, 400–404.

22) Siedle, A. R.; Newmark, R. A.; Lamanna, W. M.; Schroepfer, J. N. *Polyhedron* **1990**, *9*, 301–308.

23) It is known that the average E–Me bond energy is larger for Al compared with that of Zn (65.5 vs. 42.3 kcal/mol): O'Neill, M. E.; Wade, K. in *Comprehensive organometallic chemistry*; Wilkinson, G., Stone, F. G. A., Abel, E.W. eds; Pergamon Press, Oxford (1982).

24) Perrin, C. L.; Dwyer, T. J. *Chem. Rev.* **1990**, *90*, 935–967.

25) Petros, R. A.; Norton, J. R. *Organometallics* **2004**, *23*, 5105–5107.

26) Neuhaus, D.; Williamson, M. P. *The Nuclear Overhauser Effect in Structural and Conformational Analysis*, 2nd ed., Wiley-VCH, Weinheim, **2000**.

26) Ivanov, S. V.; Peryshkov, D. W.; Miller, S. M.; Anderson, O. P.; Rappé, A. K.; Strauss, S. H. *J. Fluor. Chem.* **2012**, *143*, 99–102.

28) Bochmann, M.; Sarsfield, M. J. *Organometallics* **1998**, *17*, 5908–5912.

29) (a) Sadow, A.D.; Tilley, T. D. *J. Am. Chem. Soc.* **2002**, *124*, 6814–6815. (b) Sadow, A.D.; Tilley, T. D. *J. Am. Chem. Soc.* **2003**, *125*, 9462–9475. (c) Sadow, A.D.; Tilley, T. D. *Organometallics* **2003**, *22*, 3577–3585.

30) (a) Walker, D. A.; Woodman, T. J.; Hughes, D. L.; Bochmann, M. *Organometallics* **2001**, *20*, 3772–3776.

31) Tonzetich, Z. J.; Schrock, R. R. *Polyhedron* **2006**, *25*, 469–476.

32) http://copasi.org/

33) http://mestrelab.com/software/